Liquid Crystals
Publication details, including instructions for authors and subscription information:
http://www.informaworld.com/smpp/title~content=t713926090

Wetting behaviour of 5CB and 8CB and their binary mixtures above the isotropic transition

M. A. Zaki Ewiss Corresponding author[a]; G. Nabil[a]; Stefan Schlagowski[b]; Stephan Herminghaus[b]
[a] Department of Physics, Faculty of Science, University of Cairo, Giza, Egypt [b] Department of Applied Physics, Ulm University, D-89069 Ulm, Germany

Online publication date: 12 May 2010

To cite this Article Ewiss Corresponding author, M. A. Zaki , Nabil, G. , Schlagowski, Stefan and Herminghaus, Stephan(2004) 'Wetting behaviour of 5CB and 8CB and their binary mixtures above the isotropic transition', Liquid Crystals, 31: 4, 557 — 566
To link to this Article: DOI: 10.1080/02678290410001666048
URL: http://dx.doi.org/10.1080/02678290410001666048

LIQUID CRYSTALS, VOL. 31, NO. 4, APRIL 2004, 557–566

Taylor & Francis
Taylor & Francis Group

Wetting behaviour of 5CB and 8CB and their binary mixtures above the isotropic transition

M. A. ZAKI EWISS*, G. NABIL
Department of Physics, Faculty of Science, University of Cairo, Giza, Egypt

STEFAN SCHLAGOWSKI and STEPHAN HERMINGHAUS
Department of Applied Physics, Ulm University, D-89069 Ulm, Germany

(*Received 30 April 2003; in final form 31 October 2003; accepted 31 October 2003*)

High resolution optical microscopy techniques have been employed to study the wetting properties of $(5CB)_x/(8CB)_{100-x}$ ($x = 0$, 10, 30, 50, 70, 90, and 100 wt %) binary mixture liquid crystal thin films above the isotropic transitions. Dewetting is found to occurr at $T_w = 65$ and 42.5°C for the 5CB and 8CB samples, respectively, and to depend strongly on the 5CB content in the mixtures. First-order wetting transitions were seen for pure 5CB and 8CB samples; a higher order wetting transitions were obtained for the mixtures. For thin film 5CB, a large hysteresis ($\Delta T = 30$°C) between wetting and dewetting during the heating and cooling is obtained. This hysteresis is compared with the corresponding values obtained for pure 8CB and mixture samples. Evidence of the formation of nematic layers on the surface of isotropic droplets was found. Attempts to extract values of the contact line tension for these materials are made. In this respect the applicability of the modified Young's equation is questionable.

1. Introduction

Wetting phenomena are related to the absorption and spreading of liquids on a solid substrate, and include the concepts of partial (and complete) wetting, and partial (and complete) drying. In recent years many investigations have been aimed at understanding the mechanisms and the stability of the wetting and spreading of liquid crystals (LCs) on a solid substrate. Various experimental techniques have been used, such as high resolution polarizing optical microscopy (HRPM), scanning polarization force microscopy (SPFM), atomic force microscopy (AFM), ellipsometry, and X-ray techniques [1–4].

The study of the wetting of a LC on an isotropic silicon substrate (coated with an evaporated silicon oxide layer about 2 nm in thickness) shows potential for industrial applications [1]. Such surfaces are known to promote a quasi-planar anchoring of nematic liquid crystals, while anchoring at the air–nematic free interface is homeotropic. Silicon wafer substrates facilitate the study of LC thin films under elastic stress due to the opposing anchoring conditions at the interfaces [5]. The study of wetting behaviour in the smectic, nematic and isotropic phases provides information for testing the fundamental theories of these phenomena [6]. There are few reports on the wetting and dewetting behaviour of LCs above the isotropic transition.

In this work, we present detailed results on the wetting properties of thin films of $(5CB)_x/(8CB)_{100-x}$ ($x = 0$, 10, 30, 50, 70, 90, and 100 wt %) binary mixtures above the temperatures of their respective bulk transitions to the isotropic phase. These results have been obtained using high resolution optical microscopy techniques.

2. Theory

For liquid droplets on solid surfaces, a certain contact line determines the wetted portion of the solid surface where the three phases—solid (s), liquid (l) and vapor (v)—are in contact, see figure 1. According to Cahn [7], each interface has a certain free energy per unit area: γ_{sl}, γ_{sv} and γ_{vl}. These parameters describe the energy content of the interfaces in the far field, i.e. far from contact line. In the vicinity of the contact line, there is a 'core region' around the nominal position of the contact line, where complications arise.

Let us consider a macroscopic liquid droplet of contact angle (θ_∞) resting on a solid substrate (s) where (θ_∞) is the limiting contact angle for very large lateral

*Author for correspondence; e-mail: mzewiss@hotmail.com

Liquid Crystals ISSN 0267-8292 print/ISSN 1366-5855 online © 2004 Taylor & Francis Ltd
http://www.tandf.co.uk/journals
DOI: 10.1080/02678290410001666048

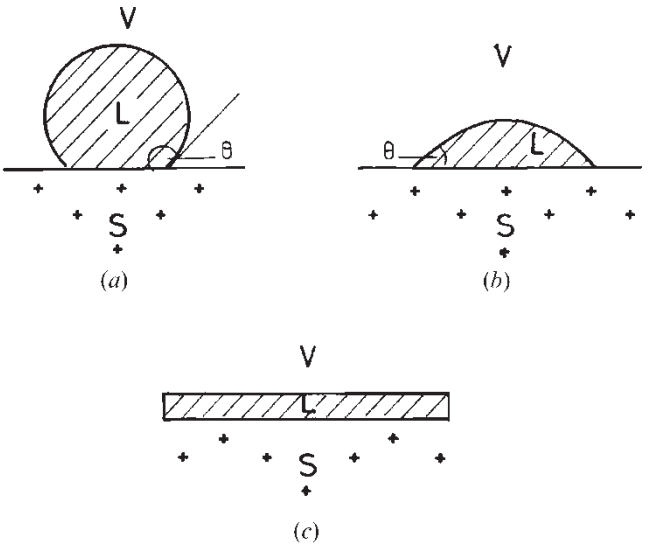

Figure 1. A small droplet in equilibrium set over a horizontal surface: (*a*), (*b*) corresponds to partial wetting, the trend towards wetting being stronger in (*b*) than in (*a*); (*c*) corresponds to complete wetting ($\theta = 0$).

radius (r). This droplet is in mechanical equilibrium with a microscopically thin adsorbed film of thickness (l_a). We have four cases:

(*a*) when $0^\circ < \theta_\infty < 90^\circ$, the substrate is partially wetted by the liquid;
(*b*) when $90^\circ < \theta_\infty < 180^\circ$, the substrate is partially dried by the liquid;
(*c*) when $\theta_\infty = 0^\circ$, the liquid wets the substrate completely;
(*d*) when $\theta_\infty = 180^\circ$, we have complete drying of the substrate by the liquid and the liquid no longer makes contact with the substrate.

It is possible to relate the contact angle (θ_∞) to the far field energies (γ_{ij}) with no knowledge of the core, since at equilibrium the energy must be stationary with respect to any shift of the contact line position. Consider a simple three-phase system, i.e. a droplet resting on a perfectly homogeneous and horizontal solid surface. If this droplet is sufficiently large so that the effect of the three-phase contact line can be neglected, the change of the free energy due to the change in the droplet size can be written as:

$$\begin{aligned} dF &= \gamma_{sl}\, dA_{sl} + \gamma_{sv}\, dA_{sv} + \gamma_{vl}\, dA_{vl} \\ &= (\gamma_{sl} - \gamma_{sv} + \gamma_{vl}\cos\theta_\infty) dA_{sl} \end{aligned} \tag{1}$$

where F is the free energy, γ is the surface free energy or surface tension, θ_∞ is the contact angle of the droplet and A is the interface area.

At mechanical equilibrium F is minimum (i.e. $dF = 0$), so we get Young's equation [7, 8]:

$$\gamma_{sv} = \gamma_{sl} + \gamma_{vl}\cos\theta_\infty \tag{2}$$

which describes the mechanical equilibrium of the forces per unit length on the three-phase contact line in the plane of the solid surface. It is worth mentioning that Young's equation (2) is strictly valid only for macroscopic droplets at mechanical equilibrium resting on a molecularly smooth horizontal solid surface.

Equation (2) also may be written as:

$$\cos\theta_\infty = \frac{(\gamma_{sv} - \gamma_{sl})}{\gamma_{vl}} = 1 + \frac{S}{\gamma_{vl}} \tag{3}$$

where, S is called the spreading parameter;

$$S = \gamma_{sv} - (\gamma_{sl} + \gamma_{vl}) \tag{4}$$

which compares the energy of the solid surface uncovered by an adsorbed film (γ_{sv}) to the energy of the substrate when covered by a thick liquid film ($\gamma_{sl} + \gamma_{vl}$).

In the condition of partial wetting, where $0^\circ < \theta_\infty < 90^\circ$ and $0 < \cos\theta_\infty < 1$, from equation (4), one gets:

$$\gamma_{sl} > \gamma_{vl} \quad \text{and} \quad S < 0 \tag{5}$$

At a certain critical temperature (T_w), the wetting temperature, below which complete wetting of the liquid thin film on the solid substrate is observed, where S decreases approaching zero, and above which the partial wetting (dewetting) of the liquid thin film from the solid surface starts,

$$\gamma_{sv} = \gamma_{sl} + \gamma_{vl}\cos\theta_\infty . \tag{6}$$

This is because the liquid/vapour interface surface tension γ_{vl} increases much faster than $(\gamma_{sv} - \gamma_{sl})$ with increasing the temperature, until reaching T_w, since the expansion rate for liquids is much greater than for solids.

From equation (4), the spreading coefficient S can be written as:

$$S = \gamma_{vl}(1 - \cos\theta). \tag{7}$$

The order of the wetting phase transition is determined by the discontinuities in derivatives of the free energy. For a wetting phase transition the singular part of the surface free energy is proportional to $(1 - \cos\theta)$, which goes to zero at T_w.

For microscopic droplets the contact angle is influenced by surface interactions, which will contribute an additional free energy per unit length or a line tension (τ) to the excess free energy of the microscopic droplet. An excess energy term will therefore be added to equation (2). Hence, for a microscopic spherical cap-shaped droplet of contact angle θ and lateral radius a,

we obtain the modified Young's equation, which can be written alternatively as [9]:

$$\gamma_{sv} = \gamma_{sl} + \gamma_{vl}\cos\theta + \frac{\tau}{a} \tag{8}$$

or

$$\cos\theta = \cos\theta_{\infty} - \frac{\tau}{\gamma_{vl}a} \tag{9}$$

where θ is the microscopic droplet contact angle, θ_{∞} is the Young's contact angle (i.e. the contact angle for an infinitely large droplet) and τ is the contact line tension which has the units of force N; γ_{vl} is the surface tension of the air/liquid crystal interface ($N\,\mu m^{-1}$) and a is the radius of curvature of the circular contact line. The quantities τ and $\cos\theta_{\infty}$ can be determined from the study of $\cos\theta$ as a function of the droplet curvature ($1/a$) at various temperatures.

3. Experimental

Figure 2 is a schematic diagram of the experimental set-up using a high resolution polarizing optical microscope (Zeiss Axiophot, coupled with a digital camera). This microscope is equipped with a hot stage (Linkam THMSG 600, temperature control better than 0.1°C). The samples were placed on the hot stage and illuminated by ordinary light emitted from a halogen lamp. This light first passes through the linear polarizer and is incident upon a quarter-wave plate through the arm of the binocular microscope. The quarter-wave plate converts the incident light to circularly polarized light. After reflection from the surface of the sample, the reflected light passes through a second quarter-wave plate. In this case the light is converted to linearly polarized light, which is 90° out of phase with respect to the incident beam. The reflected light is incident on a digital camera coupled to a video recorder. Real-time images of the film at specific temperature were recorded and displayed on the monitor. During the measurement care was taken to reduce stray light.

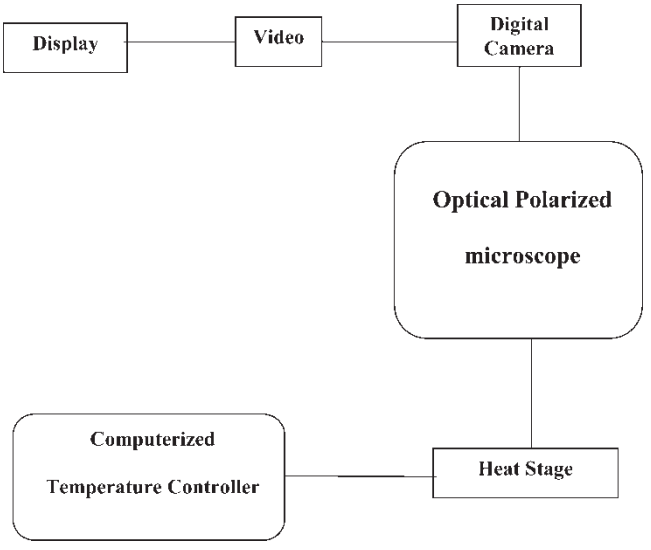

Figure 2. Schematic diagram of the dielectric experiment set-up.

The sample was observed under the polarizing optical microscope using an interference filter of wavelength $\lambda = 632\,nm$ in front of a halogen lamp. In all our measurements a magnification lens of power $\times 20$ was used, the scale calibrated such that a $1\,\mu m$ length on the sample is equivalent to 0.748 mm on the display.

In this experiment, the wetting behavior of the liquid crystals 4-*n*-pentyl-4′-cyanobiphenyl (5CB) and 4-*n*-octyl-4′-cyanobiphenyl (8CB) and their binary mixtures were studied at temperatures above the isotropic phase transition. The 5CB and 8CB were obtained from Merk KGaA (Darmstadt, Germany) and Frinton Laboratories Inc. (Vineland, NJ), respectively. In all experiments a thin layer of the sample under consideration was prepared in a class 100 clean room environment at room temperature according to the following procedure:

(1) Silicon wafers with a native oxide layer of 2 nm thicknesses (1 0 0 oriented, p-boron doped) were used as a solid substrate.
(2) The wafers were cut to about $1\,cm^2$ in size then cleaned with a snow jet of cold CO_2, effectively removing the particulate and organic contaminants; this was followed by ultrasonication in ethanol, acetone and hexane.
(3) The liquid crystal films were then spincast onto the substrate from hexane solution.
(4) The thickness of the film was controlled by the LC concentration and spinning speed of the spin-coater. The concentration of 5CB and 8CB in the hexane solution was 10.7 and $10.5\,mg\,ml^{-1}$, respectively.
(5) At a spin speed of 3000 rpm, a thickness of 50–80 nm was obtained for all samples.

The interferometry technique described above was used to study droplets formed above the isotropic phase transition for all samples. This system enabled us to measure small contact angles less than 10° with an accuracy of 0.5°–3°, for droplet radii of 1–100 μm, respectively. For all samples, the wetting behaviour was observed during heating and cooling at $0.5°C\,min^{-1}$, starting from room temperature. To avoid evaporation heating of the sample was stopped at temperatures between 60–75°C.

Dewetting of the thin isotropic film occurred above the isotropic transition and small droplets were formed.

The geometry of the cap-shaped droplet is shown in figure 3. The contact angle of each droplet is determined from the observed interference Newton's fringes by counting the number of the fringes and measuring the radius of the droplet. From figure 3, the height h of the droplet is given by

$$h=(m+0.5)\frac{\lambda}{2n} \tag{10}$$

where m is the order of the interference fringes, λ is the wavelength of the incident light and n is the refractive index of the liquid crystal sample. The contact angle θ of each droplet is calculated from the formula:

$$\theta=90^{\circ}-\cos^{-1}\left(\frac{2ah}{a^2+h^2}\right) \tag{11}$$

where a is the average radius of the spherical cap-shaped droplet.

4. Results and discussion

Bulk 5CB may exist in three phases. With increasing temperature, there is a transition at 24°C from a crystalline to a nematic (N) phase; at 33.5°C there is transition to the isotropic (I) phase. On the other hand, 8CB may exit in four different phases. With increasing temperature, there is a transition at 21°C from crystalline to smectic A (SmA) phase, another at 32.5°C to the N phase, and a third at 40°C to the isotropic I phase. 5CB molecules form dimers whose length is 25 Å, while the length of the individual molecule is 18.7 Å [2]. 8CB molecules are also paired into dimers (1.4 times longer than a single molecule) in the bulk, with antiparallel dipole moments. In the SmA

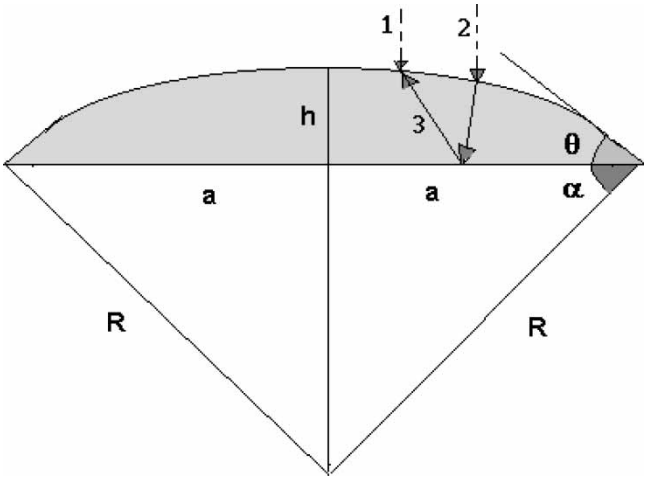

Figure 3. Sketch of a spherical cap-shaped droplet resting on a solid surface. The interference fringe is formed by the illuminating beam (1) and the reflected beam (3) originating from the illuminating beam (2). $2nh=(m+0.5)\ \lambda$; $R=(a^2+h^2)/2h$; $\cos\alpha=a/R$ since $\theta=90^{\circ}-\alpha$.

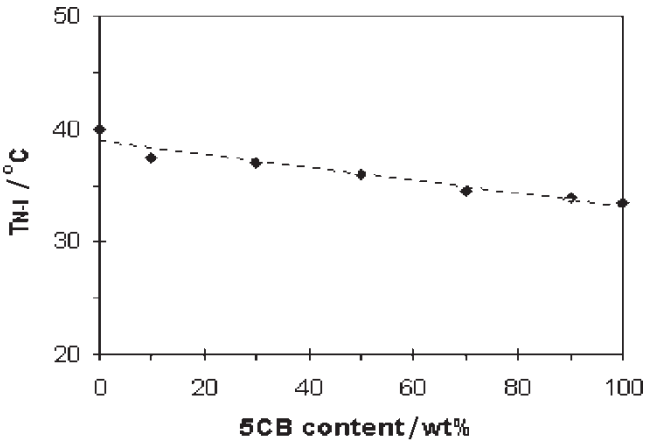

Figure 4. Phase transition temperature $T_{N\text{-}I}$ as a function of the 5CB content in the mixtures.

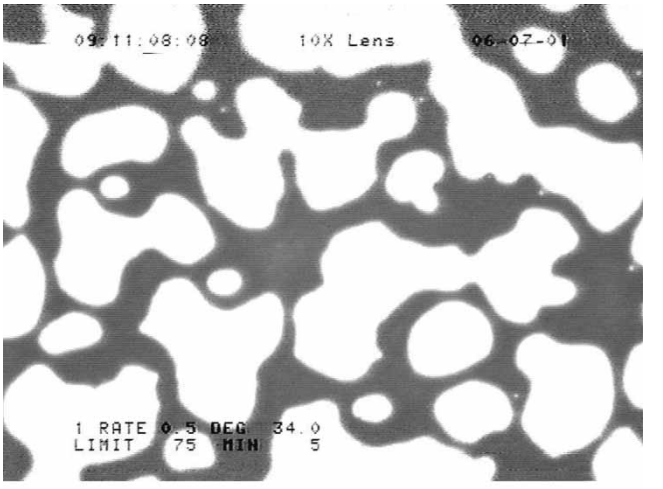

(*a*)

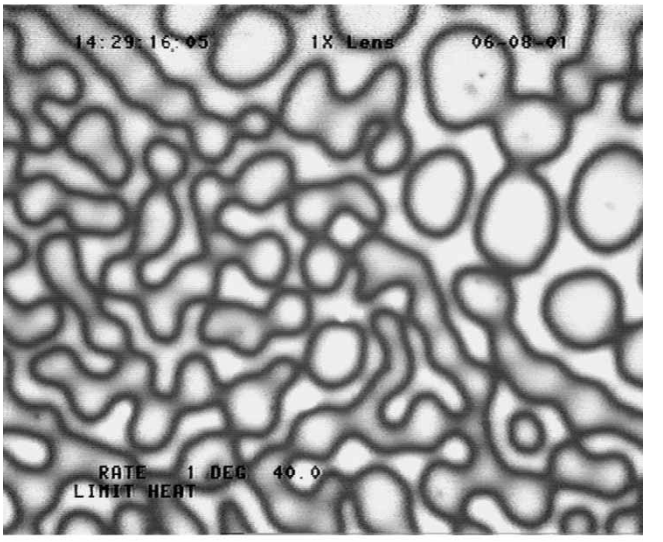

(*b*)

Figure 5. Surface undulations on approaching the nematic to isotropic phase transition: (*a*) 5CB; (*b*) 8CB.

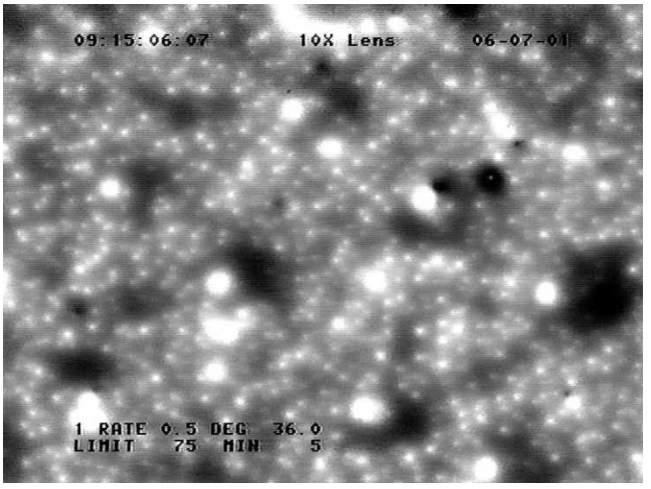

Figure 6. The white bright spot start to appear in the isotropic 5CB thin film at $T = 36^{\circ}C$.

phase the dimers form layers spaced by 31.7 Å, with the dimers aligned perpendicular to the layers [3].

In our experiment, the surface of the silicon wafer substrate promotes a quasiplanar anchoring of the *n*CB liquid crystal materials. For example, in the case of 5CB the anchoring at the air–nematic free interface is homeotropic [10]. For this reason the silicon wafer surfaces allow us to study the liquid crystal films under elastic stress (due to the opposing anchoring conditions at both interfaces).

We started the experiment by gradually heating the sample under test from room temperature ($T = 25^{\circ}C$) at a rate of $0.5^{\circ}C\,min^{-1}$. The observed phase transition temperatures from nematic to isotropic ($T_{N\text{-}I}$) phase, as determined by surface undulations [11], for all samples are shown in figure 4. These phase transition temperatures are in good agreement with the corresponding values obtained by DSC measurement [12]. It is

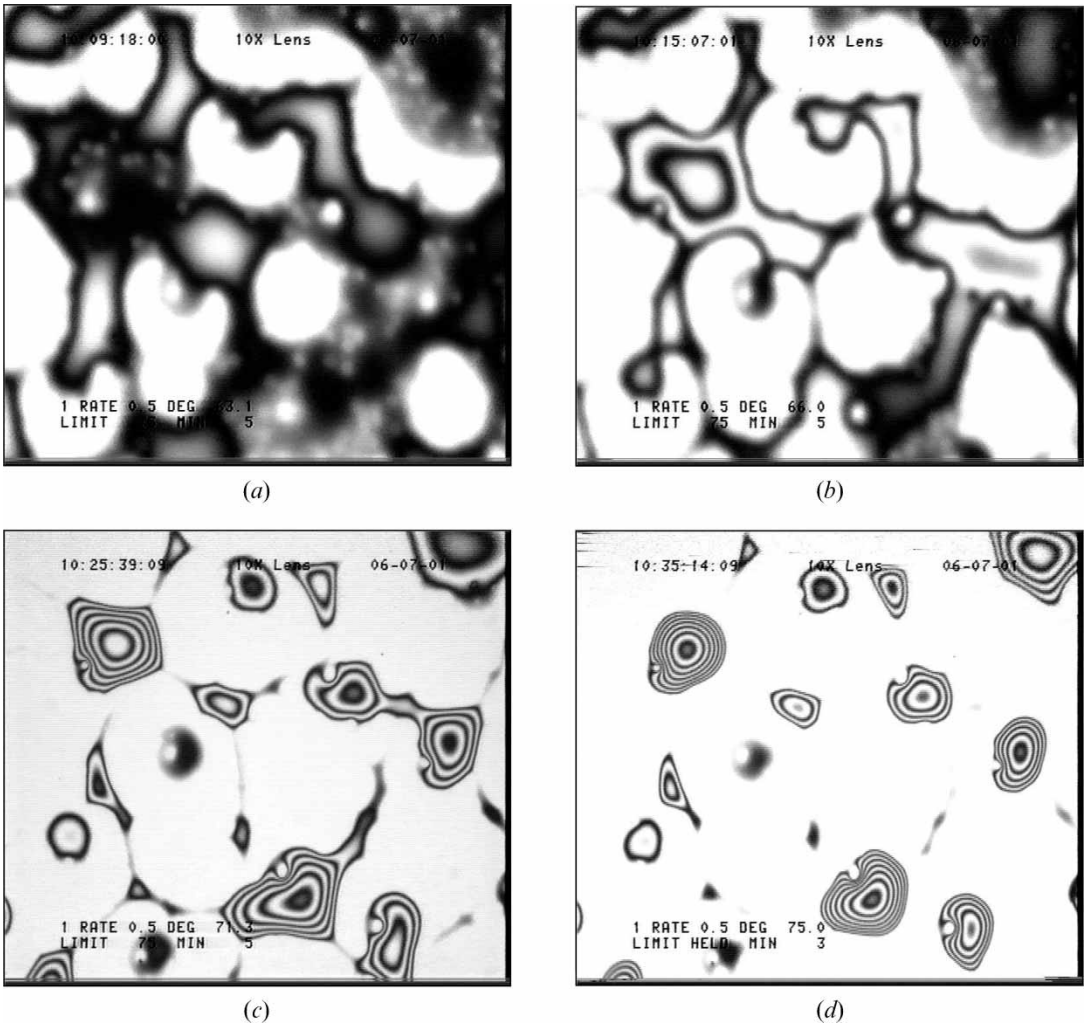

Figure 7. (*a*) White spots joined together at $T = 60^{\circ}C$; (*b*) dewetting of the isotropic 5CB thin film starts at $T = 65^{\circ}C$; (*c*) droplets start to appear but are still joining together; (*d*) the droplets are separated to form semi-spherical cap-shaped droplets.

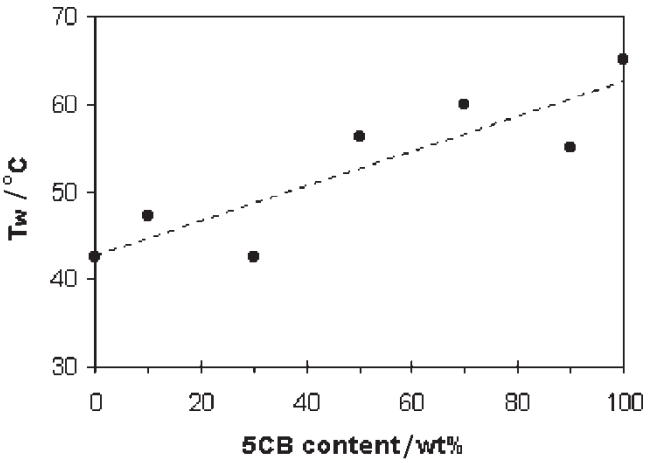

Figure 8. Variation of wetting temperature T_W with 5CB content in the mixtures.

obvious that the content of the 5CB nematic liquid crystal has an important effect on the occurrence of the SmA phase of the 8CB in the mixtures. For example, for the mixture containing 10 wt % of 5CB, the transition from SmA to nematic phase is shifted to a lower temperature at $T=27^{\circ}$C, in comparison with the corresponding value obtained for pure 8CB (at $T=32.5^{\circ}$C). For the other mixtures containing a higher 5CB content, the SmA phase vanishes completely. Approaching the nematic–isotropic transition temperature, surface undulations are observed for all samples under consideration. Figures 5 (*a*) and 5 (*b*) show the surface undulation for 5CB and 8CB, respectively. This undulation occurs due to thermally induced surface instability: an instantaneous change in the thin nematic film thickness occurs on approaching the nematic to isotropic phase transition temperature $T_{N\text{-}I}$, since some of the nematic layers (on the surface of the substrate) start the transition to the isotropic phase. The instability of this undulation has been reported previously [11, 13–17].

For the 5CB sample, at $T=36^{\circ}$C just above the phase transition temperature, a few bright spots appeared as shown in figure 6. It was noticed that on increasing the temperature the size of these spots increases. At $T=60^{\circ}$C the spots began to coalesce, then at $T=65^{\circ}$C the substrate became partially wetted by the isotropic 5CB thin film as shown in figures 7 (*a–d*). In this case small droplets were formed on the surface of the substrate with interference fringes as seen in figure 7 (*d*), where measurements were made of the radius a, with accuracy $\pm 0.1\,\mu$m for a large droplet and $\pm 0.01\,\mu$m for a small droplet ($a<20\,\mu$m), and the height h of the various droplets. Following the calculation procedure given above, the contact angle θ of each droplet was determined with an accuracy $\pm 0.01^{\circ}$. At certain temperatures the average value of the contact angle for selected droplets was considered. Figure 8 shows the variation of temperature at which the transition from complete wetting to dewetting (T_W) occurs with increasing 5CB content in the mixtures.

The variation of average contact angles θ_{av} of the droplets with temperature, during heating and cooling, for 5CB is shown in figure 9. On heating, partial wetting occurred at $T=65^{\circ}$C, and the value of the average contact angle was very small, $\theta_{av}=0.0056^{\circ}$. This value rapidly increased on increasing the temperature; it reached a value of 4.5° at $T=75^{\circ}$C. In order to avoid evaporation, the sample was not heated above 75°C. On cooling we observed no change in the shape or size

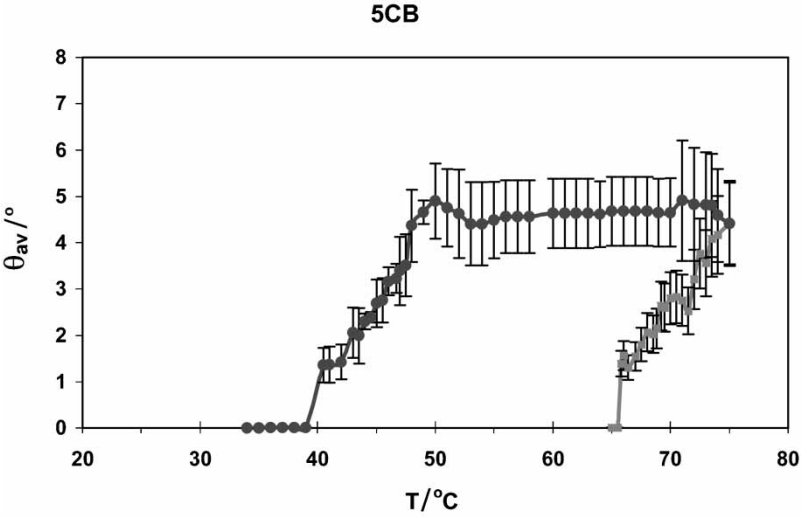

Figure 9. Variation of average contact angles θ_{av} of isotropic 5CB droplets with temperature during heating (light grey) and cooling (dark grey).

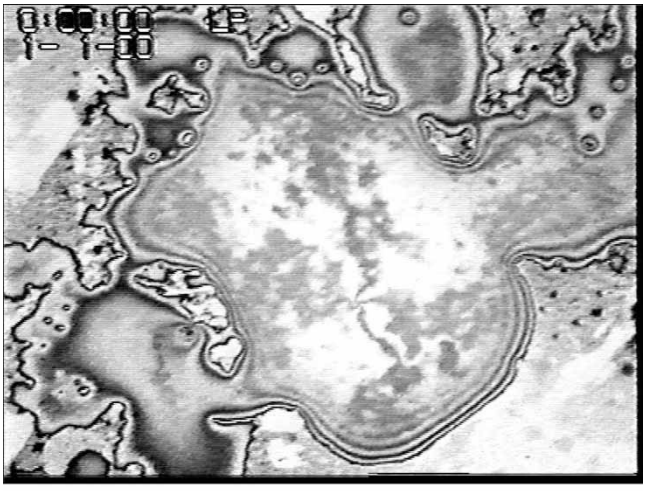

(*a*)

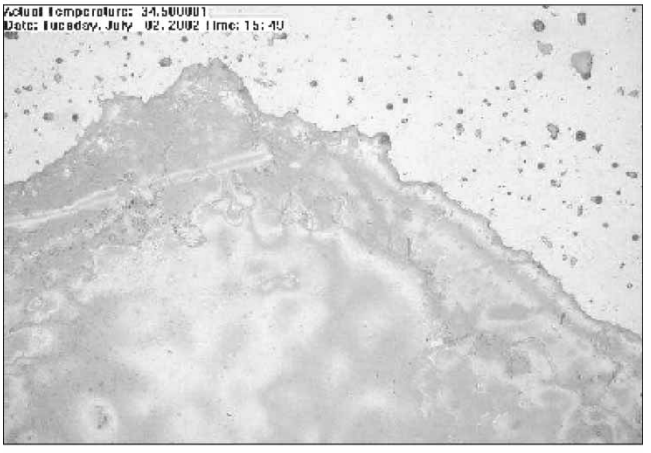

(*b*)

Figure 10. The appearance of birefringence at the surface of 5CB isotropic droplets during cooling at (*a*) $T=37.5^{\circ}$C, (*b*) $T=34.5^{\circ}$C.

of the droplet in the temperature interval 50–75°C where the value of θ_{av} is kept constant at 4.5°. On further cooling, wetting started at $T=48^{\circ}$C, where the value of θ_{av} is decreased; it reached a minimum value of 1.7° at $T=40^{\circ}$C. Surprisingly complete wetting of the surface occurred on approaching the isotropic to nematic transition temperature at $T=34^{\circ}$C. These results were reproducible on repeating the experiment several times using the same sample as well as when using fresh sample prepared under the same conditions.

In the isotropic phase at $T=37.5^{\circ}$C and $T=34.5^{\circ}$C a birefringence was observed on the top of the droplets, see figure 10. This birefringence is evidence of the presence of ordered phases at the surface of the droplets. As mentioned above, dewetting of 5CB thin film in the far isotropic phase occurred at $T=65^{\circ}$C. This value is considered to be the highest dewetting temperature in comparison with all other samples. On the other hand, from figure 9, the large hysteresis of $\Delta T=30^{\circ}$C characterizing the 5CB sample is related to the excess free energy of the droplet in the isotropic phase, compared with the corresponding energy in the nematic phase, since the surface tension in the isotropic phase is higher than in the nematic phase. This leads to instability of the isotropic film, causing partial wetting.

During cooling, the average contact angle remains constant in the temperature range 75–45°C. This is attributed to the formation of the nematic layer over the isotropic free surface discussed above. In general the formation of ordered phases on the surface of the isotropic free surface is an interesting phenomenon and has been studied using various techniques. For example, the free surface of a homologous series of low molecular mass liquid crystals *n*CB ($n=5$, 6, 7, and 8) was investigated by reflection ellipsometry by Kasten

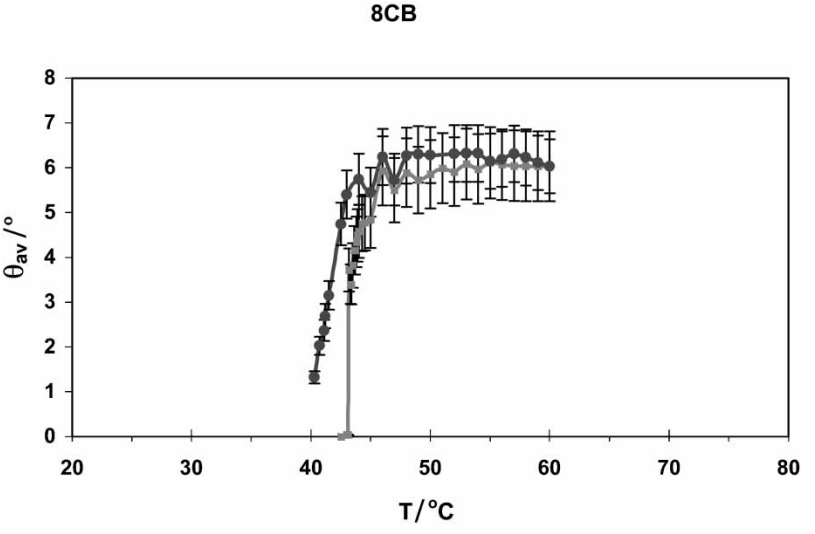

Figure 11. Variation of average contact angles θ_{av} of isotropic 8CB droplets with temperature during the heating (light grey) and cooling (dark grey).

and Strobl [18], who found that above the isotropic phase transition complete wetting by a homeotropically aligned nematic film occurs for $n=6$, 7 and 8, while for $n=5$ the wetting layer remains finite at the phase transition temperature. These previous studies support our observation of nematic layer formation on the surface of the isotropic droplets.

Concerning the smectic 8CB sample, the wetting behaviour above the isotropic transition temperature is illustrated in figure 11, where the relation between the average contact angle θ_{av} of the droplets and temperature during heating and cooling is shown. We noted that dewetting started at $T=42.5°C$, which is 35% lower than that in case of pure 5CB. At $T>42.5°C$, the value of θ_{av} rapidly increased on increasing the temperature; it reached a maximum value of 6° at $T=46°C$. In the temperature range between 46 and 60°C there was no change in the shape of the droplets; consequently the value of the average contact angle remained constant. From figure 11, on cooling the value of θ_{av} remains the same until $T=43°C$; isotropic 8CB droplets then started to spread on the silicon surface. In contrast to the 5CB sample, on further cooling to the room temperature some droplets did not spread over the surface. This wetting behavior is different from that obtained for 5CB. From figure 8, dewetting started on heating at 42.5°C, which is only 2.5°C above the clearing temperature ($T_{N\text{-}I}$). Moreover the hysteresis

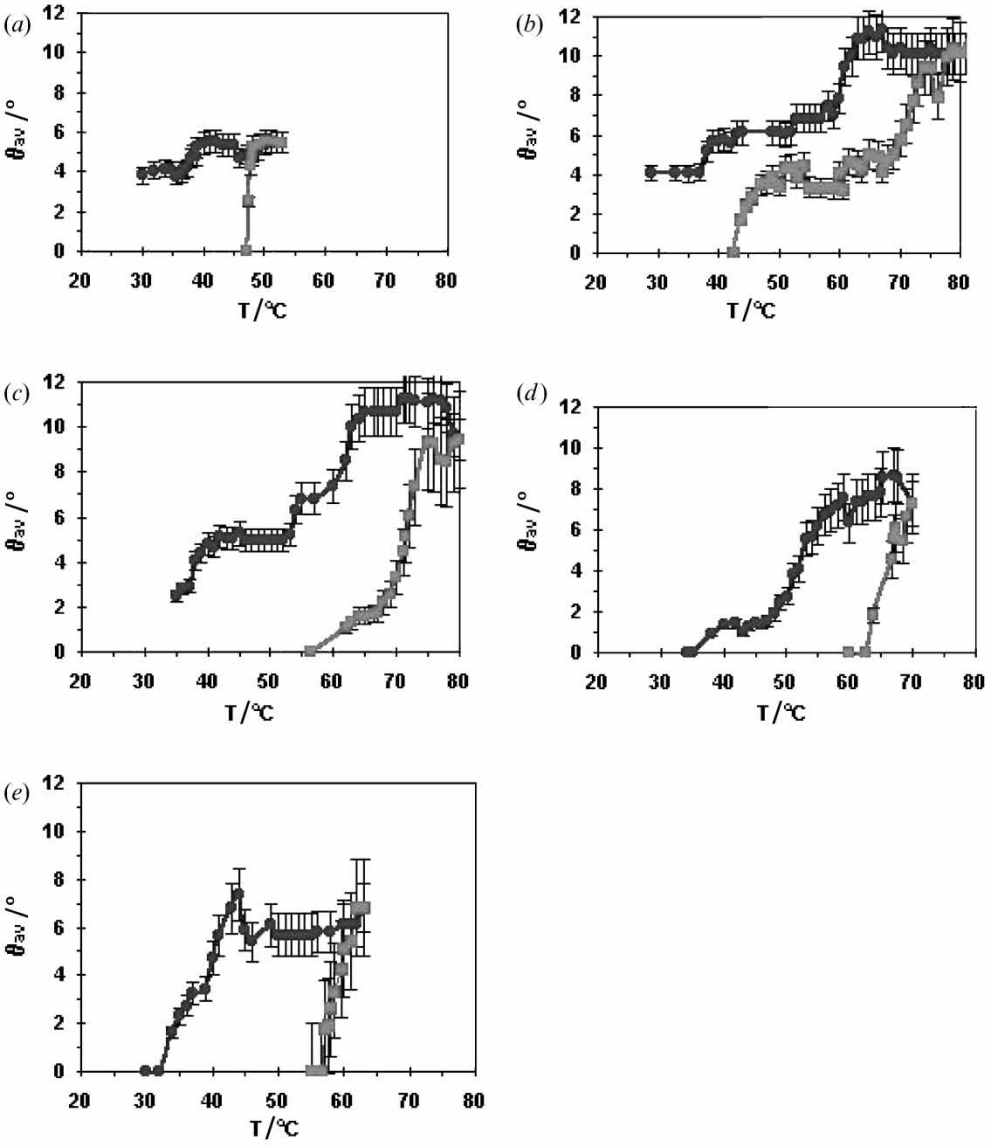

Figure 12. Variation of average contact angles θ_{av} of isotropic droplets as a function of temperature for 5CB/8CB binary mixtures, during heating (light grey) and cooling (dark grey) respectively. (*a*) 10, (*b*) 30, (*c*) 50, (*d*) 70, (*e*) 90 wt% 5CB.

between the heating and cooling was 2.6°C, which is 91% less than the hysteresis obtained for 5CB.

Similar to the case of 5CB, on cooling 8CB different ordered layers are formed above the droplets. This explains why no wetting occurred in the temperature range 60–43°C. In this respect, Xu *et al.* [3], using scanning polarization force microscopy, found evidence of the formation of a smectic layer, which partially wets the surface of the isotropic droplets. Also, Kasten and Strobl have observed the formation of a nematic layer that completely wets the isotropic surface of 8CB, using the ellipsometric technique as mentioned above [18].

The formation of these ordered layers at the surface of the isotropic droplets is related to the nature of LC materials, which are more ordered on the surface than in the bulk [4]. Furthermore, the unspread droplets remaining below the isotropic phase are related to the prewetting film, which is formed in the SmA and nematic phases during the spreading of 8CB droplets on the silicon wafer surface. The structure of this prewetting film was observed using ellipsometry and X-ray reflectivity [4] (this prewetting film is composed of a monolayer of single 8CB molecules with a thickness of 8 Å, connected to a 41 Å thick film consisting of a 33 Å thick bilayer on top of the 8 Å monolayer). For this reason, we believe that during cooling the presence of this prewetting film may hinder some droplets from further spreading on the silicon wafer surface.

We now present results on the wetting behaviour of $(5CB)_x/(8CB)_{100-x}$ binary mixtures above the isotropic phase ($x = 10$, 30, 50, 70 and 90 wt%) using the optical microscopy technique discussed above. This behaviour is illustrated in figures 12 (*a–e*) showing the effect of increasing the content of the 5CB nematic liquid crystal in the mixtures.

During both heating and cooling, changes in the wetting and dewetting transition temperatures are observed with increasing 5CB content, see figure 8. For example, on heating the mixture containing 90 wt% of 5CB, dewetting started at 55°C, which is 10°C lower than the value for pure 5CB. On cooling this mixture, wetting occurred at 30°C, compared with 34°C for pure 5CB. From figure 12 (*e*), the hysteresis between the heating and cooling processes is found to be 27°C, which is 10% less than in the case of pure 5CB. In comparing all the samples, we found that while the hysteresis decreases with decreasing 5CB content in the mixtures, there is no systematic variation in the dewetting transition temperatures.

Figures 13 (*a–d*) show the relation between $\log \theta_{av}$ and $\log t$ [where, $t = (T - T_w)/T_w$ is the reduced temperature] during heating and cooling for 5CB and 8CB. Following equation (9), it is difficult to distinguish between the order of the wetting phase transitions during heating and cooling. In this case there are no critical exponents in the usual sense, which are useful in characterizing the behaviour close to the transitions. The causes of hysteresis are not well understood in liquid crystal materials. The apparent hysteresis may

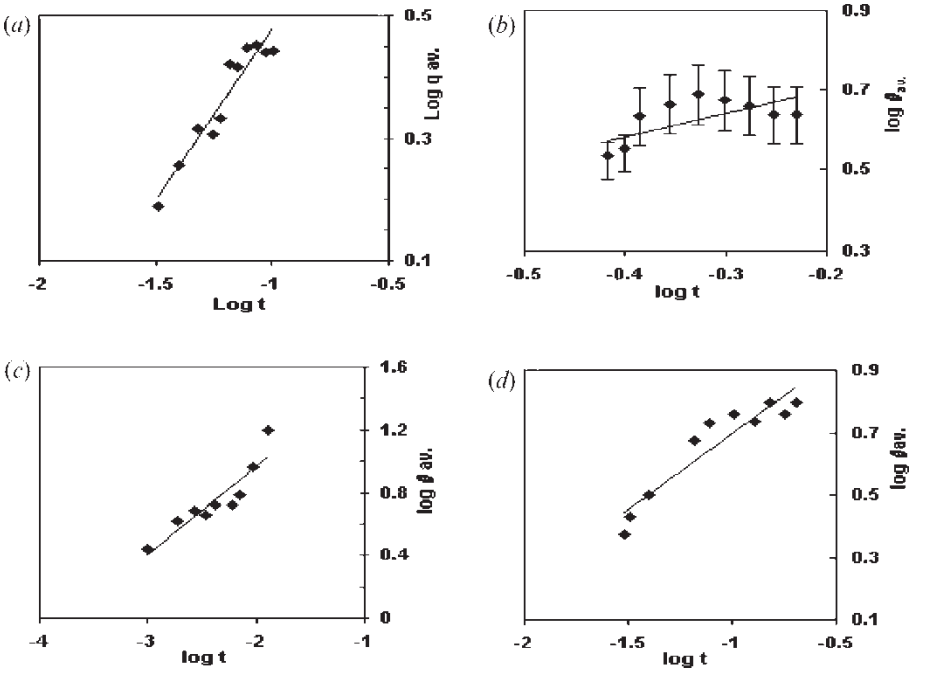

Figure 13. The logarithmic relation between the average contact angles θ_{av} and the reduced temperature, $t = (T - T_w)/T_w$, for: (*a*) 5CB during heating; (*b*) 5CB during cooling; (*c*) 8CB during heating; (*d*) 8CB during cooling.

generally be attributed to thermal gradients and the thermal history of the sample under investigation. The situation in case of 5CB/8CB binary mixtures is more complicated.

From the results presented in figures 9, 11 and 12, we see that the contact angles of the droplets are influenced by surface interactions. An earlier similar observation on other systems has been attributed to an additional free energy per unit length via equations (8) and (9). In the modified Young's equation (9) the effect of the line tension is described for real liquids. Based on this modified Young's equation, attempts have been made to extract the contact line tension for all the samples. In figures 14 (*a*, *b*), the relation between $\cos\theta_{av}$ and the curvature of the droplets $1/a$ is illustrated for selective temperature ranges 50–75°C and 46–60°C for 5CB and 8CB, respectively. From this relation, the contact line tension was found to be 6×10^{-10} N for 8CB, see figure 14 (*b*). This value is of the same order of magnitude as for real liquid samples [19, 20]. On the other hand, the modified Young's equation was not applicable to 5CB, see figure 14 (*a*). This conclusion has been discussed by Rey [21]. He tried to make a further modification for the Young's equation involving the three-phase nematic contact lines. Extra terms were added to take account of bending and anchoring forces between the liquid crystal molecules.

At this point we believe that new theoretical models dealing with the mathematical variation of the tensorial spreading parameter (which characterizes the liquid crystalline phases as functions of all involved forces) are required to explain the wetting and dewetting behaviour of such complicated systems having various mixed phases.

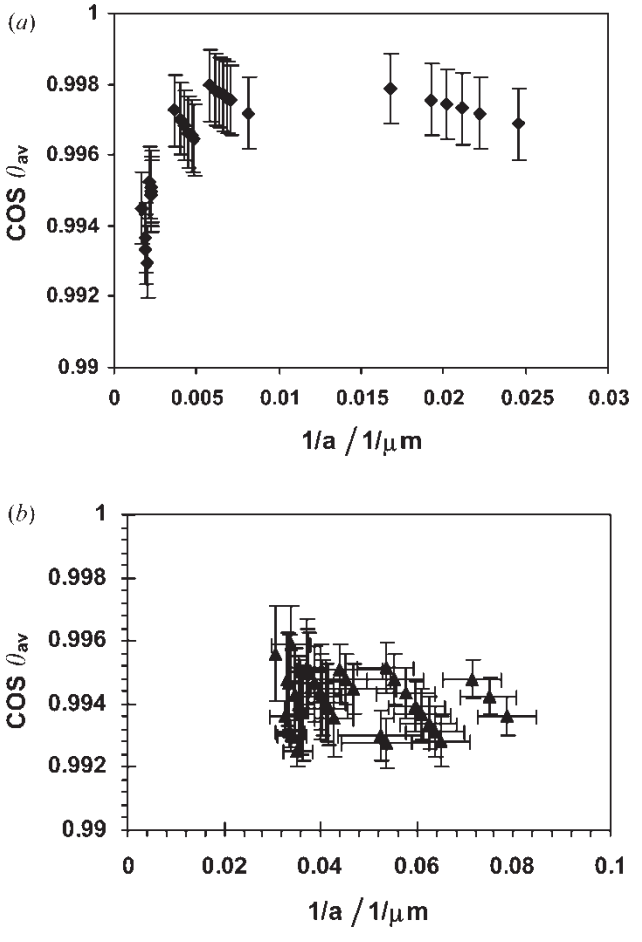

Figure 14. Relation between the cosine of the average contact angles, $\cos\theta_{av}$, and the droplet curvatures, $1/a$ for (*a*) 5CB, (*b*) 8CB.

References

[1] Collings, P. J., and Hird, M., 1997, *Introduction to Liquid Crystals, Chemistry and Physics* (London: Taylor & Francis).

[2] Vandenbrouck, F., Bardon, S., Valignat, M. P., and Cazabat, A. M., 1998, *Phys. Rev. Lett.*, **81,** 610.

[3] Xu, L., and Salmeron, M., 2000, *Phys. Rev. Lett.*, **84,** 1519.

[4] Bardon, S., Valignat, M. P., Cazabat, A. M., Stocker, W., and Rabe, J. P., 1998, *Langmuir*, **14,** 2916.

[5] Yokoyama, H., Kobayashi, S., and Kamei, H. J., 1987, *J. appl. Phys.*, **61,** 4501.

[6] Schick, M., 1990, *Introduction to Wetting Phnomenon* (Amsterdam: Elsevier Science).

[7] Cahn, J. W., 1977, *J. chem. Phys.*, **66,** 3667.

[8] Ross, D., Bonn, D., Posazhennikova, A. I., Indekeu, J. O., and Meunier, J., 2001, *Phys. Rev. Lett.*, **87,** 176 103.

[9] Rusanov, A. J., 1996, *Surface Sci. Rep.*, **23,** 173.

[10] Valignat, M. P., Villette, S., Li, J., Barberi, R., Bartolino, R., Dubois-Violette, E., and Cazabat, A. M., 1996, *Phys. Rev. Lett.*, **77,** 1994.

[11] Schlagowski, S., 2002, Dissertation, Universität Ulm.

[12] Hassanein, G. N., 2003, MSc thesis, Faculty of Science, University of Cairo.

[13] Schlagowski, S., Jacobs, K., and Herminghaus, S., 2002, *Europhys. Lett.*, **57,** 519.

[14] Vandenbrouck, F., Valignat, M. P., and Cazabat, A. M., 1999, *Phys. Rev. Lett.*, **82,** 2693.

[15] Braun, F. N., and Yokoyama, H., 2000, *Phys. Rev. E*, **62,** 2974.

[16] Herminghaus, S., Jacobs, K., Mecke, K., Bischof, J., Fery, A., Ibn-Elhaj, M., and Schlagowski, S., 1998, *Science*, **282,** 916.

[17] Herminghaus, S., Fery, A., Schlagowski, S., Jacobs, K., Seemann, R., Gau, H., Mönch, W., and Pompe, T., 1999, *J. Phys., condens. Matter*, **1,** A57.

[18] Kasten, and Strobl, G., 1995, *J. chem. Phys.*, **103,** 6768.

[19] Herminghaus, S., Pompe, T., and Fery, A. J., 2000, *Adhesion Sci. Technol.*, **14,** 1767.

[20] Pompe, T., and Herminghaus, S., 2000, *Phys. Rev. Lett.*, **85,** 1930.

[21] Rey, D., 2000, *Liq. Cryst.*, **27,** 195.